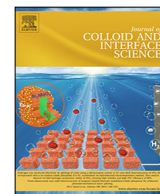Contents lists available at ScienceDirect

Journal of Colloid and Interface Science

journal homepage: www.elsevier.com/locate/jcis

Regular Article

Insight into the surface composition of bimetallic nanocatalysts obtained from microemulsions

C. Tojo [a,*], D. Buceta [b], M.A. López-Quintela [b]

[a] *Departmento de Química Física, Universidade de Vigo, E-36310 Vigo, Spain*
[b] *Laboratorio de Magnetismo y Nanotecnología, University of Santiago de Compostela, E-15782 Santiago de Compostela, Spain*

G R A P H I C A L   A B S T R A C T
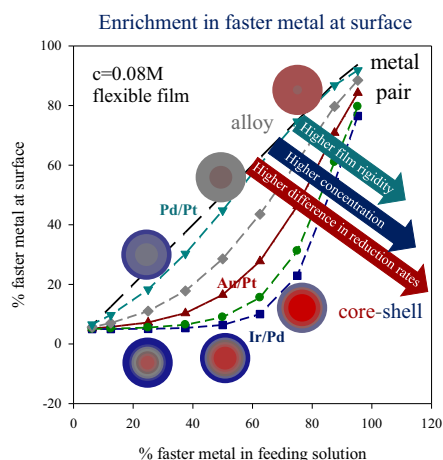
A R T I C L E   I N F O

A B S T R A C T

The enhancement of catalysts efficiency of bimetallic nanoparticles depends on the ability to exert control over surface composition. However, results relating surface composition and feeding solution of bimetallic nanoparticles synthesized in microemulsions are controversial and apparently contradictory. In order to comprehend how the resulting surface can be modified under different synthesis conditions and for different pairs of metals, a computer simulation study was carried out. The resulting surface compositions are explained based on the relative rates of deposition of the two metals, which depend on the particular metal pair, the concentration of reactants and the microemulsion composition. This study provides a satisfactory understanding of experimental results and allows us to identify the main factors affecting the nanoparticle's surface composition. Consequently, concrete and practical guidelines can be established to facilitate the experimental synthesis of bimetallic nanoparticles with tailored surfaces.
© 2021 The Authors. Published by Elsevier Inc. This is an open access article under the CC BY-NC-ND license (http://creativecommons.org/licenses/by-nc-nd/4.0/).

∗ Corresponding author.

E-mail addresses: ctojo@uvigo.es (C. Tojo), david.buceta@usc.es (D. Buceta), a.lopez@nanogap.es (M.A. López-Quintela).

1. Introduction

Bimetallic nanocatalysts are gaining increasing attention owing to their catalytic performance greater than the individual monometallic nanoparticles. [1–4]. It results in a growing interest in the tailoring of bimetallic nanostructures with desired morphologies and properties. The enhanced catalytic performance of bimetallic nanoparticles is attributed to the electronic factor, by which electrons can move from one metal to another due to partially filled d-band. The different electron density of the two metals favors the electron deficiency sites resulting in bimetallic nanocatalyst more catalytically active than the monometallic ones. These much improved catalytic activity is reflected in the increasing advance in this field, so a number of bimetallic catalysts were widely studied in different chemical reactions (see Table 1 in reference [5]).

The improvement of bimetallic particles as nanocatalysts is restricted by the possibility to design and tune the available active sites. Synthesizing bimetallic nanocatalysts that show highly particular characteristics requires an advanced control of the preparation method. Thus, the optimization of strategies to obtain bimetallic nanoparticles are still under investigation. A main aspect to be highlighted is the control of the surface composition since adsorption and desorption of reactants, intermediates and products take place on the nanocatalyst surface. Thereby the enhancement of catalysts efficiency depends on the ability to exert control over surface composition [6–10]. Furthermore, the optimal surface composition is conditioned by the particular chemical process. As a case in point, in order to catalyze electro-oxidation of methanol, Au/Pt mixed at the nanocatalysts surface were proved to improve catalytic performance [11]. Quite the contrary, catalytic activity of Au/Pt in oxygen reduction reaction [12,13] and formic acid electrooxidation [14] has been shown to be better when a Pt shell is covering the Au core.

So great efforts are put in the development of methods to synthesize efficient bimetallic nanocatalysts with highly specific composition at the surface. We will focus on one particular technique among the available methods to produce nanoparticles, that is, reactions in water-in-oil microemulsions. This is one of the most commonly used synthetic techniques, because the surfactant-stabilized reversed micelles provide a nanoreactor to obtain nanoparticles by exchanging their contents via fusion-redispersion processes. The chemical reaction take place within a nanoreactor, which favours the formation of catalysts in the nano-size range with narrow size distribution. Micelles not only facilitate reactions but also provide steric stabilizer hereby inhibiting aggregation of the synthesized particles. It leads to a control of the particle size, which -in principle- could be achieved by varying the water-to-surfactant molar ratio, that is, controlling the size of the reversed micelles. The resulting particles obtained in such a medium are usually very fine and monodisperse [15]. At the same time, the microemulsion's route offers additional advantages, such as working at room temperature, in contrast to traditional techniques that often need high temperatures [16], and that the materials synthesized in such nanoreactors can be directly applied as nanocatalysts with improved catalytic properties [16]. All these advantages make the microemulsion route one of the favorite synthetic methods for preparing bimetallic nanoparticles. So in the last years the progress in this field has been extraordinary and many pairs of bimetallic nanocatalysts have been obtained from microemulsions [16,17].

However, in spite of these advantages, the complexity inherent of the reaction medium makes a better understanding of the microemulsion method difficult, due to the limited knowledge of managing the material intermicellar exchange. The material exchange between micelles strongly influences the synthesis, because reactants are initially located in different micelles, so all stages of the procedure (reaction, nucleation and growth to build up final particles) depend on the material exchange. The rate of the intermicellar exchange is dictated by the microemulsion composition, mainly by the surfactant, whose lipophilic portion is anchored into oil and the hydrophilic one into water, leading to a film surrounding the micelle surface. The intermicellar exchange of material is allowed when the surfactant film breaks up (due to an energetic enough micelle-micelle collision), forming an intermicellar channel which enables material to cross from one micelle to another. This means that the exchange rate between micelles governs chemical kinetics in microemulsions and, as a consequence, the resulting nanostructure.

The composition of the final bimetallic particles obtained after reduction obeys to the initial ratio of the metal precursors inside micelles [16]. As a an example, Guobin et al. [18] synthesized Pd/Ag nanoalloys in a n-octane/Brij/water microemulsion whose composition was in good agreement with that of the two metal precursors in the feed solution. However, if we focus our attention on the nanoparticle surface, results relating surface composition and feeding solution are controversial. Thus, Ag/Ni core–shell nanocatalysts obtained from microemulsions showed that the molar ratio of Ni and Ag precursors seems to control the thickness of Ni layers on the surface of Ag cores [19]. At the same time, Ag/Pd nanoparticles synthesized by Sun et al. [20], in a n-butanol/CTAB/water microemulsions, showed that stoichiometric ratios between the two metals at surface match well with the molar ratios of metal salts in initial aqueous solution. Following this line, the surface composition of Pd/Pt [21] and Au/Pt [22] nanoparticles prepared in a water/AOT/isooctane microemulsion was found to vary linearly with the initial ratio of the metal precursors in feeding solution. But these results are contrary to those reported by Szumelda et al. [23], who obtained Pd/M (M = Au, Pt, Ru, Ir) nanocatalysts from microemulsions with a different extent of surface segregation, depending on the metal. They observed that, for Pd/Pt and Pd/Ir, the relation between the surface composition and the feeding solution was not linear [24].

Summarizing, studies on the surface composition of bimetallic nanoparticles prepared from microemulsions are scarce and frequently contradictory, so an enormous trial- and error- effort is needed to tune the nanoparticle surface composition. In this paper, we carried out a computer simulation study in order to deeply understand how a change in the initial metals ratio can affect the resulting surface under different synthesis conditions and for different pairs of metals. This knowledge would provide a satisfactory understanding of the experimental results and also would identify the main factors affecting the nanoparticle surface. For this purpose, the simulation model can be used to establish concrete and practical guidelines to facilitate experimental trials on the synthesis of bimetallic nanoparticles with tailored surfaces. The validity of the model predictions was previously demonstrated by comparing experimental and simulation results of Au/Pt nanoparticles [12].

An in-depth kinetic study that relates the difference in reduction rates and the final nanoarrangements was previously carried out for reactants ratio 1:1 [25]. In the paper at hand, we extended studies to show how the surface composition of the nanoparticles change with different reactants ratios and to understand it from a mechanistical point of view. The resulting surface composition is explained on the basis of the relative rates of deposition of the two metals. Thus, simultaneous deposition favours the mixture of the metals during the whole process, resulting in a surface composition similar to the feeding one. On the contrary, different deposition rates give rise to more segregated nanostructures, whose

surface composition does not match with the feeding one. Three main factors affecting the deposition rates are: the reduction kinetic constants of the two metals, the concentration of reactants, and the intermicellar exchange rate. Finally, the model results are compared to the experimental ones and the main guidelines to allow a fine tune of the surface composition are described.

2. Brief description of the simulation model

The simulation model has managed to recreate the kinetic course of the chemical reaction inside micelles (see reference [25] for details). Briefly, the microemulsion is described as a set of micelles, which contain one kind of reactant (reductor R or metal salts A^+ and B^+). Each kind of reactant is initially distributed throughout micelles using a Poisson distribution. Thus, in order to study different metal salts proportions at a fixed metal concentration, a 75% A (faster reduction metal) implies than initial microemulsions contain 24 metals salt A and 8 metal salt B (slower metal), respectively, giving rise to an averaged concentration $\langle c \rangle$=16 reactants/micelle.

Micelles move and collide with each other. In previous studies the microemulsion micelles were randomly located on a lattice with a φ% portion of the space occupied by micelles. Then, micelles performed random walks to nearest neighbor sites. Two micelles collided when they moved into contiguous lattice sites. In order to save computation time, the collision description was improved by choosing randomly two colliding micelles, which fuse, exchange material if possible, and then redisperse. By repeating this procedure of random choice of two colliding micelles, the collision dynamics of a micelles distribution that follows a Brownian motion is reproduced. Both procedures give similar results, but the second one is less time consuming. To make the connection between the two procedures, a volume fraction of micelles $\varphi = 10$% means that 1000 micelles are located in a 10,000 positions in the lattice, which is equivalent to consider 1000 micelles that collides 100 times by Monte Carlo step. Hence, to simulate an effective collision, 10% of 15,000 micelles are chosen at random to fuse and establish a channel between micelles that permits the exchange of material. This means that a $\varphi = 10$% of volume is occupied by micelles. The material carried by colliding micelles is modified after each collision obeying to the following criteria:

Exchange parameter k_{ex}: Metal precursors (A^+, B^+), reducing agent (R) and free metal atoms (A and/or B) can be exchanged between colliding micelles in accordance with the concentration gradient principle (material diffuse from the more to the less occupied micelle). The maximum number of reactants/atoms that can be transferred during a collision is quantified by the exchange parameter k_{ex}.

Flexibility parameter (f): Nanoparticles grow by aggregation of metal atoms inside micelles. The exchange of these growing particles is restricted by the size of the channel between colliding droplets. The flexibility parameter (f) quantifies the maximum particle size that is allowed to be transferred between micelles.

Both simulation parameters controlling intermicellar exchange of material (k_{ex} and f) are closely related to the flexibility of the surfactant film, which depends on microemulsion composition [26,27].

In order to include Ostwald ripening, a tiny particle can be moved to the micelle containing a bigger one in the case that both colliding micelles are carrying particles, as long as the channel size (f) allows the exchange to be produced.

Chemical reduction occurs when the metal salt (A^+ and/or B^+) and the reductor (R) are located inside the same micelle, as a result of intermicellar redistribution of material during a collision. Different reduction rates are considered by varying the percent-

age of the metal precursor carried by colliding micelles that will be reduced. Due to its instantaneous reduction rate, $AuCl_4^-$ reduction is simulated by 100% of Au salt within the colliding micelles (v_{Au} = 100%), provided that there are enough number of reductors present. Based on standard reduction potentials, the reduction rate of $PtCl_6^{2-}$ will be slower. Experimental results on Au/Pt nanoparticles by simultaneous reduction of $AuCl_4^-$ and $PtCl_6^{2-}$ with hydrazine in a isooctane/tergitol/water microemulsion were successfully reproduced by considering a 10% reduction rate for Pt [12], that is, only 10% of Pt salt inside colliging micelles gives rise to products (v_{Pt} = 10%). Reactants, which did not react (metal salts and reductor), stay in the micelle. They can be exchanged and react during a posterior collision. This correlation between the standard potentials of the two metals and reduction rates obeys to the general believe, according to which the higher the difference between the standard potentials, the higher the ratio between both reductions rates is. It is interesting to note that a change in reductor would affect to reduction rates ratio because the driving force is the ΔG of the reaction, which is proportional to the difference $\varepsilon_{reductor}$–$\varepsilon_{metal\ salt}$. For the simultaneous reduction of two metal salts, a change in $\varepsilon_{reductor}$ does not affect the difference ΔG_1-ΔG_2, but it does change the ratio $\Delta G_1/\Delta G_2$, giving rise to a different reduction rates ratio. The key is not the absolute rate of each metal, but the relative rates of the two metals and their interplay with the microemulsion dynamics. Specifically, higher reduction rate ratios woud lead to a larger metal segregation in the final nanoparticle.

Microemulsion composition dictates the micellar dynamics, that is affected by changing the surfactant, the cosurfactant and the chain length of the oil phase. A basic characteristic of a surfactant film is its flexibility, that is, its ability to depart from the optimal curvature. As a function of the interaction strength at the interface, surfactants are flexible or rigid. Rigid surfactants have a very hydrophilic headgroup and very hydrophobic long alkyl chain, so they strongly adsorb at interface decreasing the interfacial tension. Flexible surfactants easily allow curvature fluctuations. The curvature elasticity of the interface is responsible for the formation of a fused dimer (that implies an inversion of the film curvature), that is required for material intermicellar exchange. This phenomenon is included in the model by relating the flexibility of the surfactant film around the droplets and the stability and the size of the channels communicating colliding micelles. So, microemulsion composition is included in the model by means of the intermicellar exchange parameters described above. Thus, material can be exchanged between micelles whenever two requirements are met. First, colliding micelles have to stay together long enough to allow reactants diffusion go through the intermicellar channel. That is, if the two colliding micelles stay together longer, a higher amount of material is exchanged (and quantified by the k_{ex} parameter). This is the crucial parameter when the exchanged species are isolated ones (metal salts, reductor and metal atoms), that cross the channel one by one. In this case, the size of the channel is not important. Second, the channel size communicating both micelles has to be large enough to allow the growing particle to cross the channel. So, if the exchanged specie is a particle (an aggregate of metal atoms), it has to be exchanged as a whole, and f parameter restricts its exchange. In this way, a microemulsion with a high flexible surfactant film will be described by a large k_{ex} (longer dimer stability) and large f (large intermicellar channel size). That is, a more flexible film will allow the exchange of a higher quantity of reactants/atoms and larger particles than a rigid one. As a case in point, a microemulsion with a flexible film, such as isooctane/tergitol/water, was successful reproduced by combining $f = 30$ (only particles composed by less than 30 units can cross the channel) with $k_{ex} = 5$ (less than 5 free atoms can be exchanged per collision) [12].

Nanoparticle formation starts from a nucleus, which grows by deposition of atoms until becomes a particle. In the case of bimetallic particles, the sequence of deposition of the two metals will determine the degree of mixture in the resulting nanostructure. So each simulation is run until the synthesis finishes, i.e., material inside micelles remains unchanged, which means that all metal salts are reduced and intermicellar exchange is not taking place. As a result, each run ends in a set of micelles, each of them can contain a particle whose composition is different from each other. To monitor the particle composition, the sequence of the two metals deposition of each nanoparticle is stored as a function of time, and finally divided into ten concentric layers, assuming a spherical arrangement. Averaged nanoparticle composition (%A) and dispersion are calculated layer-by-layer. Lastly, results are averaged over 1000 runs.

It was proposed that the surfactant adsorption can stop the growth of the nanoparticles within the droplets, but it is not the general behavior. Although the surfactant adsorption can be important at the later stages of growth, there is no evidence that adsorption was as fast as the nanoparticle growth, even in microemulsions. Metal-metal interaction is much stronger than metal–surfactant interaction, so it can be expected that surfactant adsorption does not dominate during the early stages of the synthesis, but at the final stages.

The simulation was validated by direct comparison with experimental results (see reference [12] for details). Au/Pt particles were synthesized in a water/tergitol/isooctane microemulsion and characterized using HR-STEM and cross-sections scanned with EDX analysis to study the nanostructure. A good agreement was obtained when comparing both experimental and STEM profiles calculated from the simulated structures.

3. Results and discussion

3.1. Dependence of the surface composition on the difference in reduction rates of the two metals

First of all, we will focus on the simple approach of varying the initial reactants ratio inside micelles and analyze the resulting surface composition. A set of experiments was carried out at different concentrations and using a flexible film. The averaged outer layer composition of resulting structures was calculated as percentage of the faster reduction metal. This procedure was repeated for different pairs of metals, where the faster metal reduction was always 100% (all reactants inside colliding micelles give rise to products, if

there is enough reducing agent) and the reduction rate of slower one was decreased from 50% to 3%. This means that one of the metals has a very fast reduction rate (such Au or Ir), and the second one is slower, simulating in this way different Au/Metal couples. In all cases, the composition at the surface depends on initial molar ratio of metal salts inside micelles, but this dependence is affected by the relative reduction rates, as shown in Fig. 1A, B and C, which show results for three different reactants concentrations inside micelles. As expected, pairs with not so different reduction rates (see 100%, 50%) lead to an almost linear relation between the initial feeding composition solution and final surface composition (see dashed black line). This is the case of Ag/Pd nanoparticles synthesized in a *n*-butanol/CTAB/water microemulsion [20] and Pd/Pt nanoparticles obtained from a water/AOT/isooctane microemulsion [21]. In these experiments, the ratios between the two metals at surface match well with the ratios of metal precursors in initial feeding solution. This is because quite similar reduction rates promote the simultaneous deposition of both metals from the beginning, so it will lead to a mixed nanostructure, covered by a mixed surface, whatever the reactants ratio is. It is clearly observed in histograms in Fig. 2(A–C), which show the composition layer by layer for a pair characterized by (100,50) reduction rates at 1:4, 1:1 and 4:1 ratio in feeding solution for an averaged concentration ⟨c⟩= 16 reactants/micelle, corresponding to data shown in the upper line in Fig. 1B. However, as the difference between reduction rates of the two metals increases, the behaviour moves further away from the linear tendency, and this is more remarkable as the reduction rate of the second metal is slower. The explanation is that if the reduction of the second metal is very slow, the faster one accumulates in the inner layers, and then the slower one deposits forming the outer ones. It results in a core–shell structure, in which the amount of faster metal that reaches the surface is smaller than in feeding solution, giving rise to a large deviation from the linear tendency in the Fig. 1. This metal segregation can be clearly observed in Fig. 3, which show histograms at 1:4, 1:1: and 4:1 ratios at ⟨c⟩= 16 reactants/micelle for a couple with reduction rates (100,3), which corresponds to data shown in the lower line in Fig. 1B. One can conclude that the more similar the reductions rates are, the more similar the composition surface to feeding solution is.

Note that the deviation from the linear tendency as the difference in reduction rates depends on the reactants ratio (compare Fig. 1A, B and C). To explain this result behaviour, not only reduction rates but also the amount of reactants and the intermicellar exchange rate must be taken into account. All these parameters are included when calculating the overall reaction rate of each
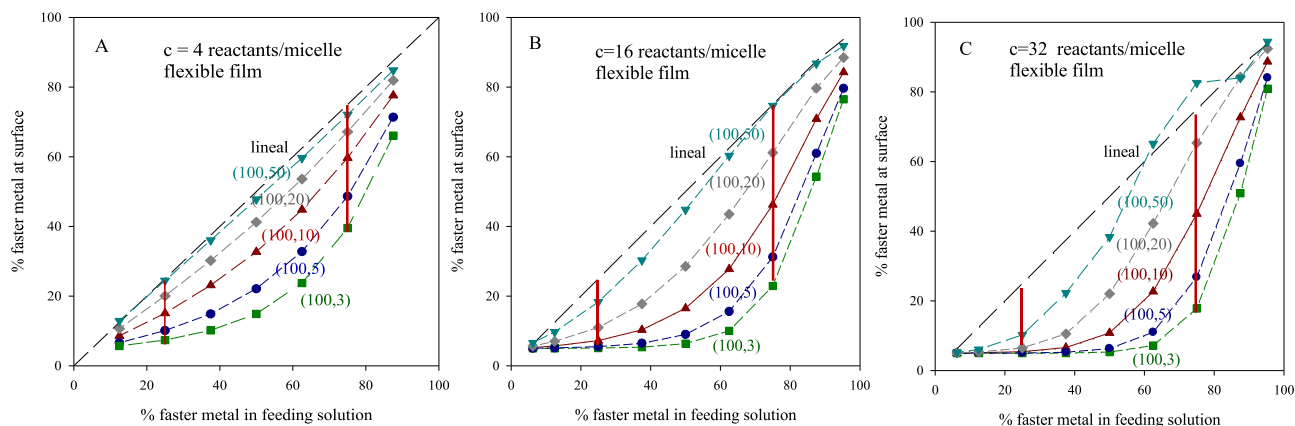

Fig. 1. % of faster metal at surface versus % faster metal in feeding solution. Reduction rates: $v_{faster\ metal}$ = 100%, $v_{slower\ metal}$ = 3, 5, 10, 20, 50%, ⟨$c_{reductor}$⟩ = 20 ⟨$c_{metal\ salt}$⟩], flexible film (f = 30, k_{ex} = 5). Lines are only guides to the eye.
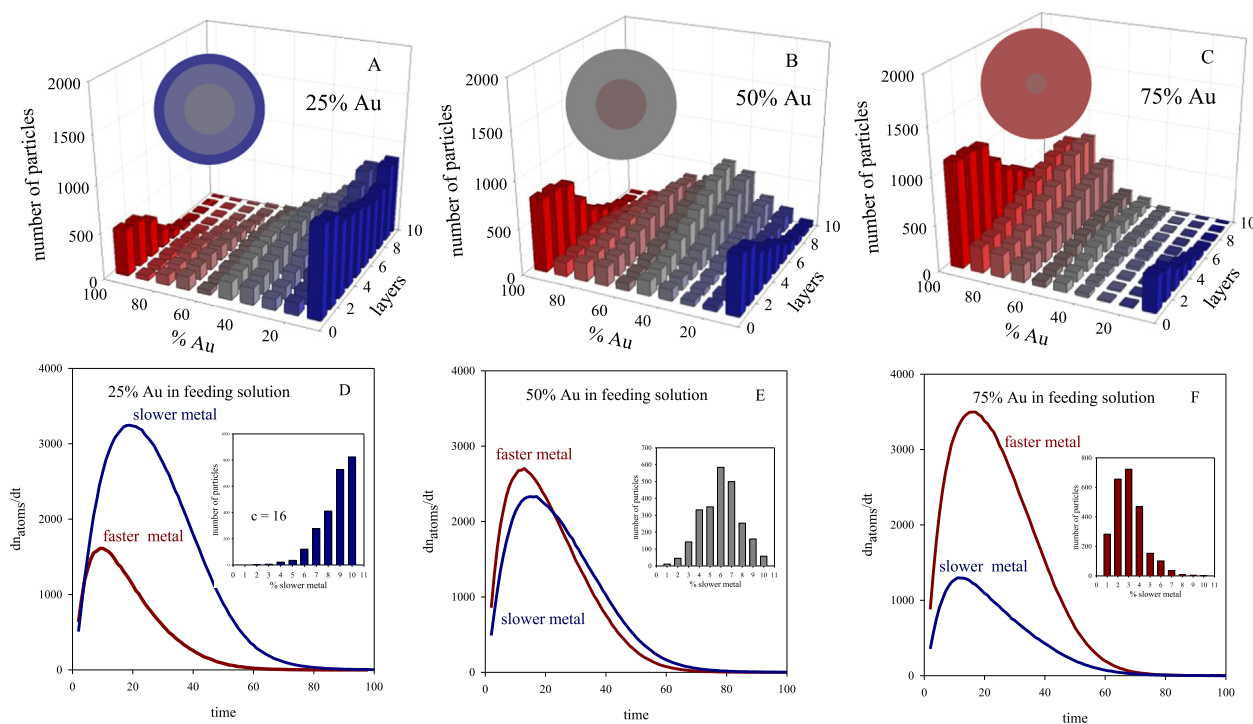
Fig. 2. A, B, C Histograms show results for 1:4, 1:1 and 4:1 reactants ratio in feeding solution. Color pattern: red is the faster metal, blue is the slower one, grey is 50%. As the color turns to lighter tonalities, the proportion of pure metal in the layer is higher. C, D, F show reaction rate calculated as dn_{atoms}/dt versus time for 1:4, 1:1 and 4:1 reactants ratio in feeding solution. Inner picture in each figure show the surface composition distribution. Reduction rates: $v_{faster\ metal}$ = 100%, $v_{slower\ metal}$ = 50%, $\langle c \rangle$ = 16, $\langle c_{reductor} \rangle$= 20 $\langle c \rangle$; flexible film (f = 30, k_{ex} = 5). The concentric colored spheres also represent the average nanoparticle composition. (For interpretation of the references to color in this figure legend, the reader is referred to the web version of this article.)

metal from the slopes of the representation of the number of metal atoms obtained in the micelles as synthesis advances. Second file in Fig. 2(D, E, and F) shows the reaction rates dn_{metal}/dt at different reactants ratio and an averaged concentration $\langle c \rangle$= 16 reactants/ micelle, corresponding to data shown in Fig. 1B. As expected, the reaction rates are faster as increasing metal amount in feeding solution (see red lines from the left to the right, and blue lines from right to left). For reactants ratio 1:1 (see Fig. 2E), faster metal curve is slightly higher than that of the slower one, due to the faster reduction rate of Au. As a result, both metals deposition is almost simultaneous, giving rise to an alloyed surface (see inner picture in Fig. 2E, which represents the surface composition). At 25% faster metal (1:4 ratio), reaction rate of slower metal is larger than the faster one (compare blue and red lines in Fig. 2D) due to its larger amount. Faster metal is exhausted early and can only reach the surface in a low proportion. As shown in the inner figure, surface composition match well with feeding solution composition. Finally, in a 4:1 (75% faster metal), both reduction rate and reactants amount contribute to an even faster reaction rate of Au (compare blue and red lines in Fig. 2F), which mixes with Pt resulting in an Au enriched surface.

Concerning a higher difference between reduction rates, that leads to well-defined core–shell particles, histograms in Fig. 3 (reduction rates = 100,3) show that the thickness of slower metal layers on the surface of the nanoparticles was controlled by the amount of the metal precursors (see blue bars at the right), as experimentally observed for Ag/Ni nanocatalysts [19]. The pictures below show the overall reactions rates for each reactants ratio (see Fig. 3D, E, F). In this case, the reduction of each metal take place at different stages of the whole process, that is, the faster metal is almost exhausted when the slower one is starting to be reduced.

It is reflected in the resulting surface composition, which is mainly composed by the slower metal for all reactant ratio. However, it can be observed that reactants ratio affects the surface composition: as increasing Au content, a larger amount of Au is able to reach the surface of some particles. As discussed below in a more detailed way, this is a consequence of the compartmentalization of the reaction medium.

Another aspect to be taken into consideration in Fig. 1 is that the deviation from the linear tendency as the difference in reduction rates becomes asymmetric at high Au ratio, that is, curves at different reduction rates tend to overlap at low Au content in feeding solution, but remain clearly different at high Au content. To understand this behaviour, note that a 1:1 ratio means that the rate difference between the two metals is only due to the difference in reduction rates, because both reactants content and exchange rate are the same for the two metals. However, for 1:4 ratio, the rate of the slower metal increases due to its greater amount, which can partially counteract the faster reduction of Au, resulting in less different rates. Then surface composition is closer to feeding one. The opposite is the case for 4:1 ratio, because both reduction rate and reactant amount favours an even faster reduction of Au. This is reflected in a surface composition that is more distant from the linear behaviour than that of 1:4 ratio one (compare red vertical lines at 25 and 75% Au in Fig. 1).

3.2. Dependence of the surface composition on initial reactants concentration

By comparing Fig. 1A, 1B and 1C, one can see that the deviation from the linear tendency is more pronounced as concentration increases, for all studied bimetallic couples. This behaviour is bet-
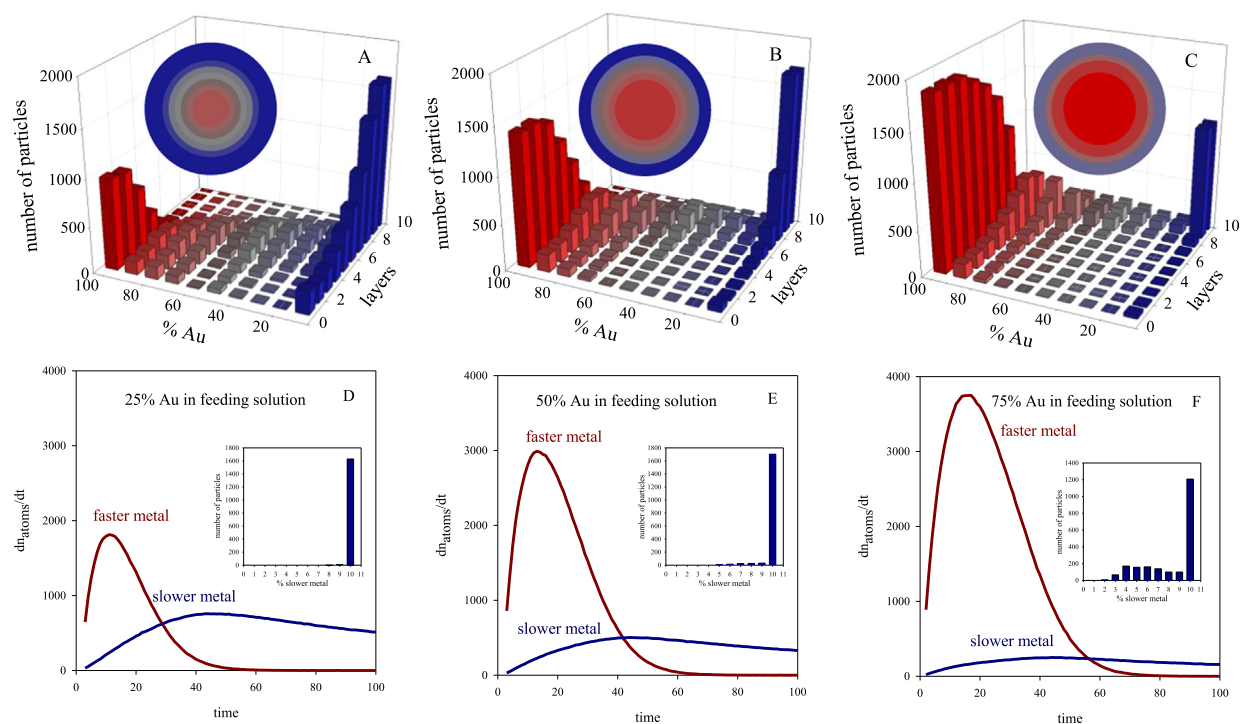
Fig. 3. A, B, C Histograms show results for 1:4, 1:1 and 4:1 reactants ratio in feeding solution. Color pattern: red is the faster metal, blue is the slower one, grey is 50%. As the color turns to lighter tonalities, the proportion of pure metal in the layer is higher. C, D, F show reaction rate calculated as dn$_{atoms}$/dt versus time for 1:4, 1:1 and 4:1 reactants ratio in feeding solution. Inner picture in each figure show the surface composition distribution. Reduction rates: v$_{faster\ metal}$ = 100%, v$_{slower\ metal}$ = 3%, $\langle c \rangle$ = 16, $\langle c_{reductor} \rangle$= 20 $\langle c \rangle$, flexible film (f = 30, k_{ex} = 5). (For interpretation of the references to color in this figure legend, the reader is referred to the web version of this article.)

ter reflected in Fig. 3A, which shows results varying concentration for a fixed metallic couple and fixed microemulsion. In all cases, the nanoparticle surface shows a progressive enrichment in the slower metal as concentration increases. Similar qualitative behaviour was found for different couples and microemulsions. It was demonstrated both experimentally and by simulation [12] that the higher the concentration the better metal segregation is, i.e., the more enriched in slower metal surface. This is mainly due to the difference in reduction rate, but intermicellar exchange must be also taken into account. From a kinetic point of view, a greater concentration implies a faster reduction, but this reasoning can be applied to both reductions. Thus, based on the hypothesis that the nanoparticle surface composition is the result of the competition between both chemical reductions, the surface composition must not be affected by initial reactants concentration, provided that both reactants concentrations are equal (considering the case 1:1 ratio). But in a compartmentalized reaction media, the intermicellar exchange controls the reactants redistribution between micelles, and consequently controls the reactants encounter and the subsequent chemical reaction. The faster metal will react as fast as the intermicellar exchange allows the reactants to encounter, so, as the synthesis advances most of the faster reduction atoms are already reduced, while the slower ones are still appearing. This delay in slow metal reduction leads to outer layers slightly enriched in Pt observed at low concentration, (see Fig. 4, surface histogram at $\langle c \rangle$ = 4). As concentration increases the quantity of slower reactants which remain in the reaction media without reacting is higher, so more intermicellar exchanges will be required to achieve the end of the synthesis. This delay in Pt reduction causes the progressive Pt enrichment at surface observed as concentration increases (see Fig. 4, surface composition histograms).

For a better understanding of the kinetic behaviour, it is important to point out the role of micelles as a dosing pump of precursors [28]: These calculations were carried out for a flexible film, whose k_{ex} value is 5, i.e., a maximum of 5 atoms can be exchanged by collision. The k_{ex} value will have a different impact depending on the occupation inside micelles. For example, for a 1:4 Au/M ratio (25% Au), the number of atoms per micelle in the feeding solution is $\langle c_{fast} \rangle$ = 8, $\langle c_{slow} \rangle$ = 24, which gives an average concentration $\langle c \rangle$ = 16 atoms/micelle. Since k_{ex} = 5 a few collisions will be required to exchange 8 atoms. On the contrary, a high number of collisions are needed to exchange reactants in highly occupied micelles, which leads to a slowdown of reaction rate. This means that micelles carrying larger metal content are more deeply affected by the restrictions dictated by the intermicellar exchange than that of less occupied micelles. Consequently, chemical reaction in more occupied micelles will take place over a longer period, so the metal will be deposited for longer stages of the synthesis, favouring that Au could reach the surface. This is observed in Fig. 1C, in which the combination of a pair with quite similar reduction rates (surface composition closer to feeding composition) with a large reactant amount (high concentration, high % Au) results in an Au enriched surface, higher than expected and higher than feeding solution (see upper line showing rates (100,50), that crosses the linear tendency at high Au%).

3.3. Dependence of the surface composition on the intermicellar exchange rate

In order to provide a deep insight into the intermicellar exchange rate effects on nanoparticle surface Fig. 5 shows results of computer simulations carried out keeping constant reduction rates ((100, 10) which corresponds to Au/Pt pair [12]) and using
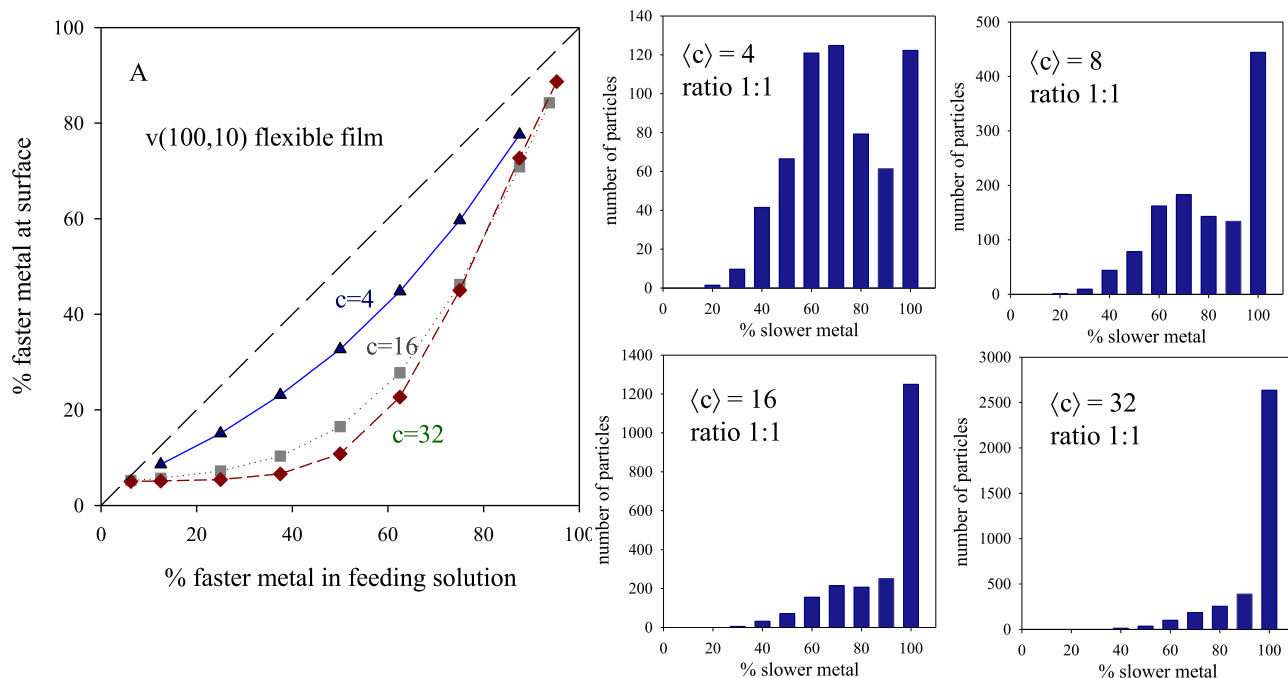
Fig. 4. % of faster metal at surface versus % faster metal in feeding solution for a fixed metal pair (characterized by reduction rates: $v_{\text{faster metal}} = 100\%$, $v_{\text{slower metal}} = 10\%$), and a fixed microemulsion composition (characterized by a flexible film ($f = 30$, $k_{ex} = 5$)), and for different initial reactants concentrations. Lines are only guidelines to the eye. Histograms show the metal distribution at the surface using different initial reactants concentrations.
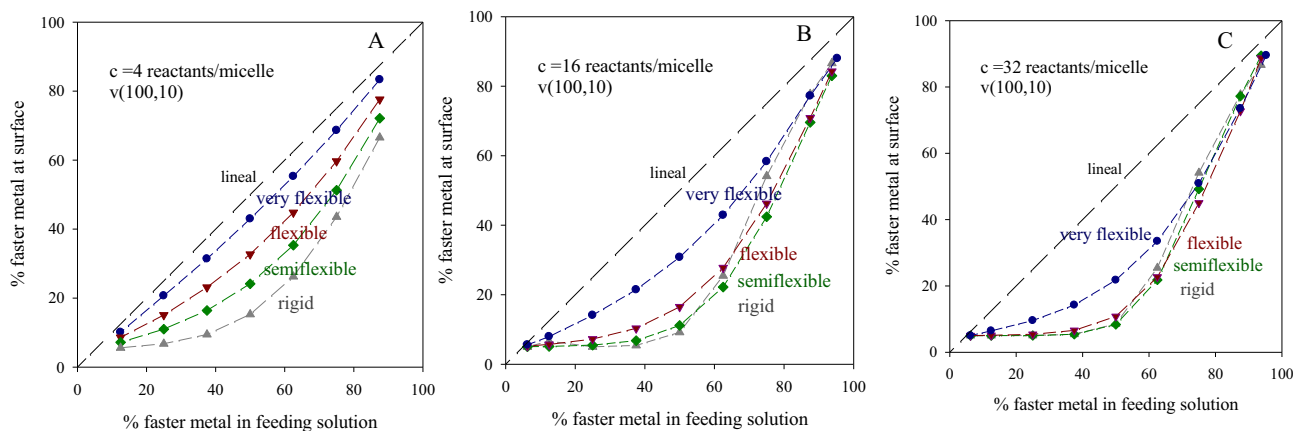

Fig. 5. % of faster metal at surface versus % faster metal in feeding solution at different film flexibilities (rigid film: $k_{ex} = 1$, $f = 5$; semiflexible film: $k_{ex} = 3$, $f = 15$; flexible film: $k_{ex} = 5$, $f = 30$; very flexible film: $k_{ex} = 15$, $f = 90$). Reduction rates: $v_{\text{faster metal}} = 100\%$, $v_{\text{slower metal}} = 10\%$. Figures A, B, and C show $\langle c_{\text{metal salt}} \rangle = 4$, 16 and 32 reactant/micelle respectively. $\langle c_{\text{reductor}} \rangle = 20 \langle c_{\text{metal salt}} \rangle$. Lines are only guidelines to the eye.

different flexibility parameters. At low concentration (see Fig. 4A), it can be observed that the more flexible the film is, the more similar the surface composition to feeding solution is. The combination of a fast intermicellar exchange and a low occupation in micelles favours the mix of reactants from the beginning. In this way, a very flexible film (faster intermicellar exchange rate) almost reproduces the result expected for a homogeneous reaction medium (a linear relationship). It was proved that better segregated structures are obtained as the intermicellar exchange rate is slower [29], which is reflected in a higher deviation from the linear behaviour shown in Fig. 5 as the film is more rigid. By observing Fig. 5B and C, two main features can be noted: First, for a given film flexibility, the deviation from linear tendency is larger at high concentration as earlier explained; second, curves at different intermicellar exchange rates approximate when increasing concentration. That is, surface composition has only marginally changed when

exchange rate is modified if concentration is high. A deeper study on this aspect will be published in detail elsewhere.

3.4. Comparison with experimental results

There are not many experimental data focusing on the study of nanoparticle surface composition at different metallic ratio using a one-pot method in microemulsions. A lineal relationship was obtained by Guobin et al. [18] who prepared Pd/Ag nanoparticles from a *n*-octane/Brij/water microemulsion. In this case, the surfactant is a rigid one, so one could expect a non-linear behaviour. But in this experiment the composition of the whole alloy, not only the surface, is represented versus the feed solution composition. When the whole nanoparticle is considered, the model always leads to a linear behaviour for any couple and any microemulsion composition.
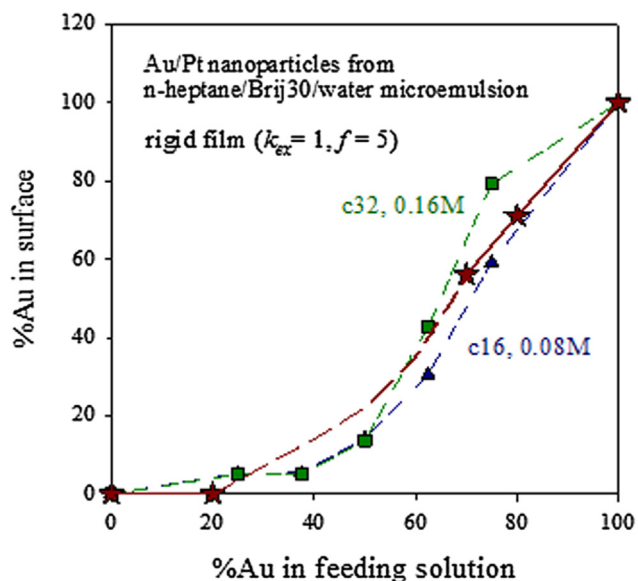
Fig. 6. %Au at the surface versus %Au in feeding solution. Synthesis conditions: rigid film (k_{ex} = 1, f = 5), ⟨c⟩ = 32 reactants/ micelle ∼ 0.16 M (green squares) and ⟨c⟩ = 16 reactants/ micelle ∼ 0.08 M (blue triangles). Stars represent experimental data of Au/Pt nanocatalysts synthesized in a *n*-heptane/Brij30/water microemulsion, taken from reference [30]. Lines are only guidelines to the eye. (With permission of RSC, reference [28]). (For interpretation of the references to color in this figure legend, the reader is referred to the web version of this article.)

Fig. 7. %Ir at the surface versus %Ir in feeding solution. Synthesis conditions: flexible film (k_{ex} = 5, f = 30), ⟨c⟩ = 32 reactants/ micelle ∼ 0.16 M (green squares) and ⟨c⟩ = 16 reactants/ micelle ∼ 0.08 M (grey squares). Stars represent experimental data of Ir/Pd nanocatalysts synthesized in a *n*-heptane/Triton-X/water microemulsion, taken from reference [24]. Lines are only guidelines to the eye. (For interpretation of the references to color in this figure legend, the reader is referred to the web version of this article.)

Stars in Fig. 6 show experimental results on the surface composition versus initial composition for Au/Pt nanoparticles obtained from a *n*-heptane/Brij30/water microemulsion [30]. In order to compare these experimental results with the nanostructures predicted by simulation, the following simulation parameter were chosen: In spite that a stronger reductor such as NaBH₄ was used in this experiment, the values of reduction rates of Au and Pt were 100% and 10% respectively, based on previous studies in which our prediction model was able to reproduce Au/Pt nanostructures synthesized by the microemulsion method [12]. In relation to the microemulsion characterization, the exchange rate parameter was k_{ex} = 1, combined with a channel size f = 5, which simulate a rigid film as provided for the surfactant Brij30. Finally, the concentration value in experiments was 0,1M. To calculate the initial number of reactants by micelle from this value of concentration, the micelle radius is required, but it is not available. Therefore, for comparison, we used a droplet radius 7,3 nm (measured in an AOT microemulsion, which is also associated to a rigid film) to calculate concentrations: ⟨c⟩ = 16 reactants/micelle ∼ 0,08 M and ⟨c⟩ = 32 reactants/micelle ∼ 0,16 M. Experimental data (0.1 M) must be between these two values of concentration. Discontinuous lines in Fig. 6 show simulation results, in which experimental results appears overlapped (see stars). One can observe that computational model reproduces satisfactorily the experimental data.

Another case of study was the preparation of Ir/Pd nanocatalysts in a microemulsion using Triton X as surfactant [24]. Because Triton–X provides of a flexible film, the parameters used to compare were k_{ex} = 5, f = 30 (flexible film). The difference between the standard reduction potential of the precursors is very high, and reduction rate of Ir is very fast, so this couple was characterized by the (100,3) reduction rates. The values of concentration are known (0.2–0.02 M), but the droplet radius was not available. So, three values of concentration are shown in Fig. 7 to test the agreement. Although the experimental data on the % of faster metal at surface are always higher than the simulated ones (see red circles), it is interesting to note that the tendency remains approximately constant until 50% faster metal in feeding solution, which is congruent with simulation data.
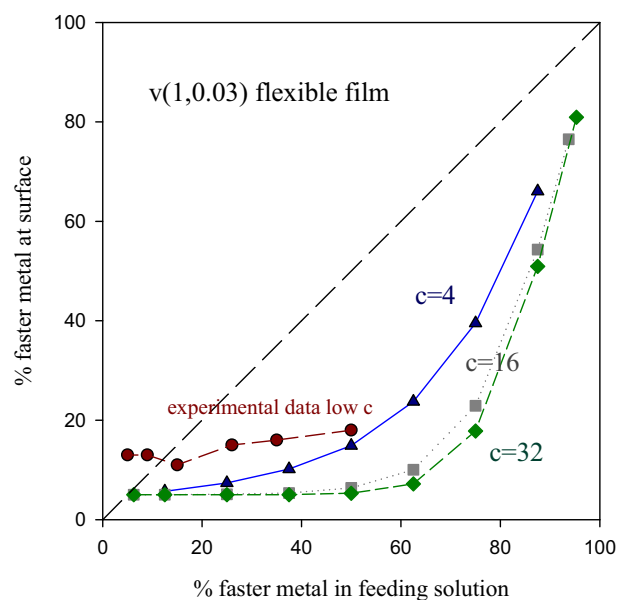
Another example is the pair Pd/Ag, which was prepared from microemulsions using CTAB as surfactant [20]. Based on the quite similar reduction potentials of Pd and Ag salts, a small difference in reduction rates can be assumed. In fact, Pd/Ag nanoparticles have been always obtained as an alloy by a one-pot method in microemulsions, which supports quite similar reduction rates. If, in addition, a very flexible microemulsion is used, such as CTAB, it is expected that the surface composition of Pd/Ag alloy was in good agreement with that of the two metal salts in the feed solution, as observed by Sun et al. [20].

4. Conclusions

The ability to exert control over surface composition of bimetallic nanoparticles is a decisive factor to improve their catalytyc activities. Nevertheless, in spite of the achievements accomplished, we still face major challenges in addressing how the surface composition can be tuned, which is crucial for the optimization and understanding their catalytic properties. Our premise is that the resulting surface composition can be explained on the basis of the relative rates of deposition of the two metals. Thus, simultaneous deposition favours the mixture of the metals during the whole process, resulting in a surface composition similar to the feeding one. In addition, different deposition rates give more segregated nanostructures, whose surface composition does not match with the feeding one. Three main factors affect the deposition rates: the reduction rate constant of the metals, the concentration of reactants and the intermicellar exchange rate. The main conclusions drawn from this study are: 1. The more similar the reductions rates, the more similar the composition surface to feeding solution is, because similar reduction rates promote the simultaneous deposition of both metals from the beginning, which leads to a mixed nanostructure, covered by a mixed surface, whatever the reactant ratio is. 2. The higher the concentration, the greater enrichment in slower metal at the surface. This is due to the combination of a compartmentalized reaction medium and different reduction rates,

which leads to a delay in slower metal reduction. Thus, the faster metal reacts as fast as it is allowed to by the intermicellar exchange, so at advanced stages of the synthesis, most of faster reactants are already reduced, while the slower ones are still at the beginning. At low concentration, this delay in slow metal reduction gives rise to a slight enrichment at the surface. As concentration increases the quantity of slower reactants that remain in the reaction media without reacting is greater, so more collisions and exchanges will be required to achieve the end of the synthesis. This larger delay in slower metal reduction causes the greater enrichment at the surface observed at high concentration. 3. The more flexible the film, the more similar the surface composition to feeding solution, because high flexibility facilitates the intermicellar exchange, favouring the mixing of reactants from the beginning. Therefore, the nanocatalyst surface can be finely tuned just by adjusting the synthesis parameters. For example, for a couple with a small difference in reduction rates, if the goal is to get a good metal segregation, with a surface enriched in the slower metal, a rigid surfactant combined with a high reactants concentration favours metal separation. On the contrary, if the pair of metals have quite similar reductions rates, but the goal is the obtention of an alloyed surface, the use of a flexible film combined with a low concentration favours a more simultaneous metals deposition. We hope that these simple guidelines can be used to fine-tune the surface composition in bimetallic nanostructure, which is of major importance in catalytic applications. Future research will be focused on a better understanding of the microemulsion ability to modify metal distribution in bimetallic nanoparticles.

Declaration of Competing Interest

The authors declare that they have no known competing financial interests or personal relationships that could have appeared to influence the work reported in this paper.

Acknowledgments

References

[1] A.B. Vysakh, C.L. Babu, C.P. Vinod, Demonstration of Synergistic Catalysis in Au@Ni Bimetallic Core-Shell Nanostructures, J. Phys. Chem. C 119 (2015) 8138–8146.

[2] A.S. Bandarenka, A.S. Varela, M. Karamad, F. Calle-Vallejo, L. Bech, F.J. Perez-Alonso, J. Rossmeisl, I.E.L. Stephens, I. Chorkendorff, Design of an active site towards optimal electrocatalysis: overlayers, surface alloys and near-surface alloys of Cu/Pt(111), Angew. Chem. Int. Ed. 51 (2012) 11845–11848.

[3] X. Gu, Z.-H. Lu, H.-L. Jiang, T. Akita, Q. Xu, Synergistic catalysis of metal-organic framework-immobilized Au-Pd nanoparticles in dehydrogenation of formic acid for chemical hydrogen storage, J. Am. Chem. Soc. 133 (2011) 11822–11825.

[4] A. Zielinska-Jurek, E. Kowalska, J.W. Sobczak, W. Lisowski, B. Ohtani, A. Zaleska, Preparation and characterization of monometallic (Au) and bimetallic (Ag/Au) modified-titania photocatalysts activated by visible light, Appl. Catal. B 101 (2011) 504–514.

[5] R.K. Rai, D. Tyagi, K. Gupta, S.K. Singh, Activated nanostructured bimetallic catalysts for C–C coupling reactions: recent progress, Catal. Sci. Technol. 6 (2016) 3341–3361.

[6] J. Suntivich, Z. Xu, C.E. Carlton, J. Kim, B. Han, S.W. Lee, N. Bonnet, N. Marzari, L.F. Allard, H.A. Gasteiger, K. Hamad-Schifferli, Y. Shao-Horn, Surface composition tuning of Au-Pt bimetallic nanoparticles for enhanced carbon monoxide and methanol electro-oxidation, J. Am. Chem. Soc. 135 (2013) 7985–7991.

[7] B.J. Hwang, L.S. Sarma, J.M. Chen, C.H. Chen, S.C. Shih, G.R. Wang, D.G. Liu, J.F. Lee, M.T. Tang, Structural Models and Atomic Distribution of Bimetallic Nanoparticles as Investigated by X-ray Absorption Spectroscopy, J. Am. Chem. Soc. 127 (2005) 11140–11145.

[8] G.A. Somorjai, J.Y. Park, Molecular factors of catalytic selectivity, Angew. Chem. Int. Ed. 47 (2008) 9212–9228.

[9] W. Yu, M.D. Porosoff, J.G. Chen, Review of Pt-based bimetallic catalysis: from model surfaces to supported catalysts, Chem. Rev. 112 (2012) 5780–5817.

[10] H. Liao, A. Fisher, Z.J. Xu, Surface segregation in bimetallic nanoparticles: a critical issue in electrocatalyst engineering, Small 11 (2015) 3221–3246.

[11] L. Zhao, J.P. Thomas, N.F. Heinig, M. Abd-Ellah, X. Wang, K.T. Leung, Au-Pt alloy nanocatalysts for electro-oxidation of methanol and their application for fast-response non-enzymatic alcohol sensing, J. Mater. Chem. C 2 (2014) 2707–2714.

[12] D. Buceta, C. Tojo, M. Vukmirovik, F.L. Deepak, M.A. López-Quintela, Controlling bimetallic nanostructures by the microemulsion method with sub-nanometer resolution using a prediction model, Langmuir 31 (2015) 7435–7439.

[13] M. Shao, A. Peles, K. Shoemaker, M. Gummalla, P.N. Njoki, J. Luo, C.-J. Zhong, Enhanced oxygen reduction activity of platinum monolayer on gold nanoparticles, J. Phys. Chem. Lett. 2 (2011) 67–72.

[14] G.-R. Zhang, D. Zhao, Y.-Y. Feng, B. Zhang, D.S. Su, G. Liu, B.-Q. Xu, Catalytic Pt-on-Au nanostructures: Why Pt becomes more active on smaller Au particles, ACS Nano 6 (2012) 2226–2236.

[15] A. Bumajdad, J. Eastoe, M.I. Zaki, R.K. Heenan, L. Pasupulety, Generation of metal oxide nanoparticles in optimised microemulsions, J. Colloid Interf. Sci. 312 (2007) 68–75.

[16] M. Boutonnet, S. Lögdberg, E.E. Svensson, Recent developments in the aplication of nanoparticles prepared from w/o microemulsions in heterogeneous catalysis, Curr. Opin. Colloid Interf. Sci. 13 (2008) 270–286.

[17] S. Eriksson, U. Nylen, S. Rojas, M. Boutonnet, Preparation of catalysts from microemulsions and their applications in heterogeneous catalysis, Appl. Catal. A 265 (2004) 207–219.

[18] W. Guobin, D. Wei, L. Qian, C. Weiliang, Z. Jingchang, Reverse microemulsion synthesis and characterization of Pd-Ag bimetallic alloy catalysts supported on Al₂O₃ for acetylene hydrogenation, China Pet. Process. Pe. 14 (2012) 59–67.

[19] L. Xia, X. Hu, X. Kang, H. Zhao, M. Sun, X. Cihen, A one-step facile synthesis of Ag-Ni core-shell nanoparticles in water-in-oil microemulsions, Colloids Surf. A 367 (2010) 96–101.

[20] X. Sun, Q. Qiang, Z. Yin, Z. Wang, Y. Ma, C. Zhao, Monodispersed silver-palladium nanoparticles for ethanol oxidation reaction achieved by controllable electrochemical synthesis from ionic liquid microemulsions, J. Colloid Interf. Sci. 557 (2019) 450–457.

[21] M. Wu, D. Chen, T. Huang, Preparation of Pd/Pt bimetallic nanoparticles in water/AOT/isooctane microemulsions, J. Colloid Interf. Sci. 243 (2001) 102–108.

[22] M. Wu, D. Chen, T. Huang, Preparation of Au/Pt bimetallic nanoparticles in water-in-oil microemulsions, Chem. Mater. 13 (2001) 599–606.

[23] T. Szumelda, A. Drelinkiewicz, R. Kosydar, M. Góral-Kurbiel, J. Gurgul, D. Duraczynska, Formation of Pd-group VIII bimetallic nanoparticles by the "water-in-oil" microemulsion method, Colloids Surf. A 529 (2017) 246–260.

[24] T. Szumelda, A. Drelinkiewicz, R. Kosydar, J. Gurgul, Synthesis of carbon-supported bimetallic palladium-iridium catalysts by microemulsion: characterization and electrocatalytic properties, J. Mater. Sci. 56 (2021) 392–1341.

[25] C. Tojo, D. Buceta, M.A. López-Quintela, Bimetallic nanoparticles synthesized in microemulsions: a computer simulation study on relationship between kinetics and metal segregation, J. Colloid Interf. Sci. 510 (2018) 152–161.

[26] S. Quintillán, C. Tojo, M.C. Blanco, M.A. López-Quintela, Effects of the intermicellar exchange on the size control of nanoparticles synthsized in microemulsions, Langmuir 17 (2001) 7251–7254.

[27] L. Chiappisi, L. Noirez, M. Gradzielski, A journey through the phase diagram of a pharmaceutically relevant microemulsion system, J. Coll. Interf. Sci. 473 (2016) 52–59.

[28] J. Pérez-Álvarez, C. Tojo, D. Buceta, M.A. López-Quintela, Tailored surface composition of Au/Pt nanocatalysts synthesized in microemulsions: A simulation study, RSC Adv. 10 (2020) 42277–42286.

[29] C. Tojo, M. de Dios, F. Barroso, Surfactant effects on microemulsion-based nanoparticle synthesis, Materials 4 (2011) 55–72.

[30] A. Habrioux, W. Vogel, M. Guinel, L. Guetaz, K. Servat, B. Kokoh, N. Alonso-Vante, Structural and electrochemical studies of Au-Pt nanoalloys, Phys. Chem. Chem. Phys. 11 (2009) 3573–3579.